Applied and Environmental Microbiology, July 2010, p. 4260–4268 Vol. 76, No. 13
0099-2240/10/$12.00 doi:10.1128/AEM.00166-10

Production of Indole from L-Tryptophan and Effects of These Compounds on Biofilm Formation by *Fusobacterium nucleatum* ATCC 25586[▽]

Takako Sasaki-Imamura,[1] Akira Yano,[2] and Yasuo Yoshida[1]*

Department of Dental Pharmacology, Iwate Medical University School of Dentistry, Morioka, Iwate, Japan,[1] and Iwate Biotechnology Research Center, Kitakami, Iwate, Japan[2]

Received 22 January 2010/Accepted 4 May 2010

The L-tryptophan degradation product indole is a purported extracellular signaling molecule that influences biofilm formation in various bacteria. Here we analyzed the mechanisms of indole production in *Fusobacterium nucleatum* and the effects of tryptophan and indole on *F. nucleatum* planktonic and biofilm cells. The amino acid sequence deduced from the *fn1943* gene in *F. nucleatum* ATCC 25586 was 28% identical to that deduced from *tnaA* in *Escherichia coli*, which encodes tryptophanase catalyzing the β-elimination of L-tryptophan to produce indole. The *fn1943* gene was cotranscribed with the downstream gene *fn1944*, which is a homolog of *tnaB* encoding low-affinity tryptophan permease. The transcript started at position −68 or −153 from the first nucleotide of the *fn1943* translation initiation codon. Real-time quantitative PCR showed that much more *F. nucleatum fn1943* transcripts were obtained from log-phase cells than from stationary-phase cells. Indole production by the purified recombinant protein encoded by *fn1943* was examined using high-performance liquid chromatography. The K_m and k_{cat} of the enzyme were 0.26 ± 0.03 mM and 0.74 ± 0.04 s^{-1}, respectively. *F. nucleatum* biofilm formation and the biofilm supernatant concentration of indole increased dose dependently with increasing tryptophan concentrations. Exogenous indole also increased *F. nucleatum* biofilm formation in a dose-dependent manner. Even at very high concentrations, tryptophan did not affect *fn1943* expression, whereas similar indole concentrations decreased expression. Thus, exogenous tryptophan and indole were suggested to increase *F. nucleatum* biofilms.

Fusobacterium nucleatum is a Gram-negative, anaerobic, nonmotile, non-spore-forming, spindle-shaped or fusiform rod bacterium that has been implicated as a causative agent of various periodontal (4, 11, 39), orofacial (5, 26), brain (8), liver (2), abdominal (6), blood (33), and gynecological (38) abscesses and infections in humans. The oral cavity is the primary colonization site of *F. nucleatum*, which is one of the most abundant anaerobes in subgingival plaque. *F. nucleatum* is an important central species in oral biofilm development, bridging early and late plaque biofilm colonizers by coaggregating with a wide array of microorganisms in the oral cavity (29). However, the mechanism driving *F. nucleatum* progression from planktonic to biofilm cells is poorly understood.

Indole has long been known as a chemorepellent with a nasty odor (54) and more recently has been shown to control the expression of several genes, including those associated with amino acid metabolism (55), plasmid maintenance (7), multidrug exporters (24), pathogenicity islands (1), and polysaccharide production (41). In addition, indole acts as a cell-to-cell signaling molecule that mediates biofilm formation in various bacteria carrying the gene for tryptophanase (also known as tryptophan indole-lyase; EC 4.1.99.1) (34, 37, 41, 54). Tryptophanase has been isolated from several bacterial species, including *Escherichia coli* (44), *Bacillus alvei* (25), *Aeromonas liquefaciens* (10), *Proteus rettgeri* (58), *Proteus vulgaris* (27), *Haemophilus influenzae* (36), and *Porphyromonas gingivalis* (61). It consists of four identical monomers, each containing one molecule of pyridoxal 5′-phosphate (PLP). The PLP molecule forms an aldimine bond with a lysine residue (31) and catalyzes the reversible hydrolytic cleavage of L-tryptophan to produce indole and ammonium pyruvate via an α,β-elimination mechanism (equation 1) (50):

$$\text{L-tryptophan} + H_2O \leftrightarrow \text{indole} + \text{pyruvate} + \text{ammonium} \quad (1)$$

The tryptophanase (*tna*) operon has been extensively studied in *E. coli* (57) and consists of a promoter-leader regulatory region (13) followed by *tnaA* encoding tryptophanase and *tnaB* encoding low-affinity tryptophan permease (Fig. 1) (18). Transcription of these two structural genes is regulated by both the catabolite repression and tryptophan-induced inhibition of Rho factor-dependent transcriptional termination in the leader region of the operon (*tnaL*) (51). The *tnaL* transcript contains a coding region for a 24-residue leader peptide (*tnaC*) followed by a Rho factor-binding site. Tryptophan induction requires the attempted translation of *tnaC*. The last sense codon of *tnaC* (a proline codon) is translated by $tRNA_2^{Pro}$ The translating ribosome retaining uncleaved TnaC-$tRNA_2^{Pro}$ stalls at the *tnaC* stop codon to block access of Rho factor to the *rut* site in the *tna* transcript, thereby preventing transcriptional termination in the *tnaL* region of the operon (19–22).

We recently reported the molecular basis for indole production in *P. gingivalis* W83 (61). Although the enzymatic proper-

* Corresponding author. Mailing address: Department of Dental Pharmacology, Iwate Medical University School of Dentistry, 1-3-27 Chuo-dori, Morioka, Iwate 020-8085, Japan. Phone: 81-19-651-5111. Fax: 81-19-651-0722. E-mail: yasuoy@iwate-med.ac.jp.

▽ Published ahead of print on 14 May 2010.

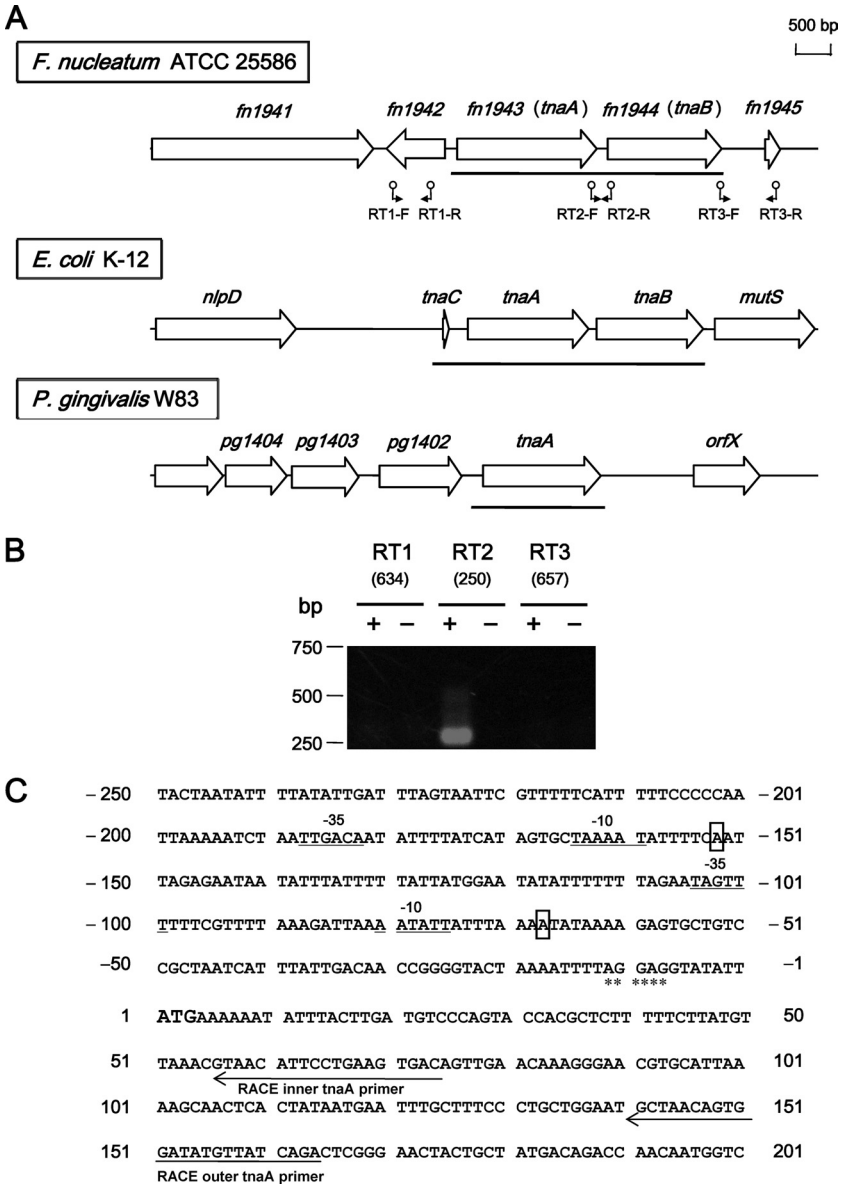

FIG. 1. Genetic organization and transcriptional analyses of the *tnaA* region of *F. nucleatum* ATCC 25586. (A) Gene arrangements of the *tnaA* region in *F. nucleatum* ATCC 25586, *E. coli* K-12, and *P. gingivalis* W83. The DNA sequence of each region was obtained from the database. Large and small arrows indicate ORF positions and RT-PCR primers, respectively. Solid bars indicate *tna* region transcripts. (B) RT-PCR analysis of *tnaA* gene expression. Total RNA was prepared from a culture in the exponential growth phase. PCR amplicons were applied to 1.2% agarose gel electrophoresis. The expected size (bp) of each PCR amplicon is shown in parentheses. Lanes marked + or − are standard RT-PCR amplifications or negative controls containing no cDNA, respectively. Positions of the DNA size standards (in bp) are indicated on the left. (C) Determination of the transcription start site by RLM-RACE. The coding region starting with ATG (large boldface) is shown with the upstream promoter region. Identified transcriptional start sites are boxed. Positions of the *tnaA*-specific outer and inner primers used for RLM-RACE are indicated by arrows. The consensus promoter sequences (23) are shown directly below the −10 and −35 regions. A Shine-Dalgarno sequence is marked with asterisks (49).

ties of tryptophanase in *P. gingivalis* were somewhat similar to those in *E. coli*, the *tnaA* regions completely differed in both genetic organization and transcriptional mechanism between the two bacteria. Unlike the flanking region of *E. coli tnaA*, no genes homologous to *tnaB* or *tnaC* were identified in the *P. gingivalis tnaA* region or elsewhere in the genome (61). Studies of the indole production mechanism have now been extended to *F. nucleatum*, a representative indole producer in oral microorganisms. In the present study, we identified and examined the expression of the tryptophanase-encoding gene in *F. nucleatum* and characterized the tryptophanase enzyme activity. The effects of exogenous tryptophan and indole on *F. nucleatum* biofilms and *tnaA* expression were also investigated.

MATERIALS AND METHODS

Bacterial strains and culture conditions. *F. nucleatum* subsp. *nucleatum* ATCC 25586 obtained from RIKEN BioResource Center (Tsukuba, Japan) was grown anaerobically at 37°C in Columbia broth (Difco, Detroit, MI). *E. coli*

TABLE 1. Oligonucleotide primers used in this study

Purpose	Primer	Sequence (5′ to 3′)[a]
RT-PCR	RT-1-F	CTCAATCTTCCCCACATATC
	RT-1-R	AGGAAAAACCTTAGGTCCATCTTT
	RT-2-F	ATAATTTACCTATGAGACACTTCC
	RT-2-R	CCAATACAAGCTAAGATGAAG
	RT-3-F	TGCACTTCTTGGAGA
	RT-3-R	GAGACAGTTCGGTAT
RLM-RACE		
	RACE outer adapter primer	GCGAGCACAGAATTAATACGACT
	RACE inner adapter primer	CGCGGATCCGAACACTGCGTTTGCTGGCTTTGATG
	RACE outer tnaA primer	AATTCATTATAGTGAGTTGCTTT
	RACE inner tnaA primer	CTGTCACTTCAGGAATGTTAC
Real-time PCR	071609-tnaA-F2	TGAACAAAGGGAACGTGCATT
	071609-tnaA-R2	ATTCCAGCAGGGAAAGCAAA
	081909-fn0654-Real-F	TGCTAAGACTGTTGTATGGAATGGA
	081909-fn0654-Real-R	ACATACTCCTATTGTTCCTTTTGCAA
	081909-fn2054-Real-F	CCCTGCTTCTGTTGACTTAACAAC
	081909-fn2054-Real-R	AGGTTTCTTCTGCCATCTTGGA
Purification of Fn1943	091708-fn-F1	AAGGATCCAAAAAATATTTACTTGATGTCCC
	110608-fn-R1	AAGTCGACCTATTTTTCTTCATTTGGATAAGG

[a] Underlined nucleotides indicate the positions of restriction endonuclease sites incorporated to facilitate cloning.

strains DH5α (Invitrogen, Carlsbad, CA) and Rosetta (Novagen, Madison, WI), used for DNA manipulation and protein purification, respectively, were grown aerobically in 2× TY broth (Difco) with 100 μg ml^{-1} ampicillin or 20 μg ml^{-1} chloramphenicol.

Extraction of RNA. Unless otherwise specified, total RNA was extracted from an *F. nucleatum* ATCC 25586 culture brought to exponential growth using FastPrep Blue tubes (Bio101, Vista, CA), as described previously (61). Contaminating DNA in the samples was eliminated by digestion with RNase-free DNase (Takara Bio, Otsu, Japan).

RT-PCR. Reverse transcriptase (RT)-mediated PCR was performed as previously described (60), with minor modifications. Briefly, RNA (5 ng μl^{-1}) was reverse transcribed into single-stranded cDNA with 0.05 ng μl^{-1} random hexadeoxyribonucleotide primers (Takara Bio) using PrimeScript Reverse Transcriptase (Takara Bio) according to the manufacturer's instructions. The gene-specific primers used for PCR are listed in Table 1. The reaction mixtures used as negative controls contained no reverse transcriptase, allowing us to evaluate the existence of contaminating genomic DNA in the samples.

RLM-RACE. RNA ligase-mediated rapid amplification of cDNA ends (RLM-RACE) was used to determine the transcription start site of *tnaA* in *F. nucleatum* ATCC 25586 with total RNA. Rapid amplification of the 5′ cDNA ends was performed using a FirstChoice RLM-RACE kit (Ambion, Austin, TX) according to the manufacturer's instructions. Briefly, a 45-base RNA adapter was ligated to the RNA population using T4 RNA ligase. This RNA population was then used as a template for a random-primed reverse transcription reaction. The cDNA product was used as a template for PCR using a *tnaA*-specific outer primer (RACE outer *tnaA* primer) and a reverse primer to the adapter (RACE outer adaptor primer). The PCR conditions were as follows: 94°C for 3 min; 35 cycles of 94°C for 30 s, 60°C for 30 s, and 72°C for 30 s; and 72°C for 5 min. The identity of the product was confirmed using inner gene-specific primers (RACE inner *tnaA* primer and RACE inner adaptor primer). *E. coli* was transformed with the amplicon ligated into an intermediate-copy-number vector, pMCL210 (42). Plasmids isolated from 11 colonies were sequenced, and sequences were analyzed using Vector NTI software (Invitrogen).

Real-time quantitative PCR analysis. Overnight cultures of *F. nucleatum* ATCC 25586 were diluted (1/50) in fresh Columbia broth and then incubated for 4, 8, 12, or 24 h. Cell growth was monitored by determining the optical density at 595 nm (OD_{595}), and the cells collected at each incubation point were used for RNA extraction.

To evaluate the effect of tryptophan or indole on *tnaA* expression in *F. nucleatum* ATCC 25586, either material was added to the cell culture that had been incubated for 8 h, and the cells were incubated for another 1 h. RNA obtained from the cultures was reverse transcribed into single-stranded cDNA with random primers, as described above. Real-time quantitative PCR amplification, detection, and analysis were performed using the Thermal cycler Dice RealTime system (Takara Bio) with Power SYBR green PCR master mix (Applied Biosystems, Foster City, CA). A reaction mixture for real-time PCR (25 μl) contained 1× Power SYBR green PCR master mix, 22.5 pmol of each forward and reverse primer, and 2.5 μl of cDNA template. The reaction conditions were 95°C for 10 min, followed by 40 cycles of 95°C for 15 s and 60°C for 1 min. At the end of each run, a dissociation protocol (95°C for 15 s, 60°C for 30 s, and 95°C for 15 s) was performed to ensure that nonspecific PCR products were absent. Two constitutive housekeeping genes, the phosphoglycerate kinase gene *fn0654* and glucose-6-phosphate isomerase gene *fn2054*, were used as internal standards to normalize for the amount of total RNA in each sample (47). The primers used in real-time quantitative PCR (Table 1) were designed using Primer Express software (version 3.0; Applied Biosystems).

To estimate the initial amounts of template in each sample, serial real-time PCRs were performed using the purified genomic DNA of *F. nucleatum* ATCC 25586. For each gene, a standard curve was plotted using the log of the initial quantity of template against the threshold cycle (i.e., the cycle at which the fluorescence rose above the background level). Data were obtained from four independent experiments.

Purification of recombinant tryptophanase. The recombinant tryptophanase of *F. nucleatum* ATCC 25586 was purified using the expression vector pGEX-6P-1 (GE Healthcare, Piscataway, NJ) as previously described (59). The coding sequence of *fn1943* was PCR amplified with KOD DNA polymerase (Toyobo, Osaka, Japan) from the genomic DNA of *F. nucleatum* ATCC 25586 using the primers listed in Table 1. The amplicons were purified and ligated into the pGEX-6P-1 vector via the BamHI and SalI restriction sites juxtaposing the *fn1943* gene, which is downstream from the coding sequence for glutathionine *S*-transferase (GST) and a PreScission protease cleavage site. *E. coli* Rosetta cells were transformed with the resulting plasmid, pGER100-3, after the correctness of the amplification of the 1,635-bp insert was verified by sequencing.

Production cultures (500 ml) were inoculated 1:100 with an overnight culture and grown to an OD_{595} of 0.7 at 30°C. The cell culture was incubated at 30°C for 1.5 h with 0.2 mM isopropyl-β-D-thiogalactoside (IPTG) to induce protein expression, and the cells were harvested by centrifugation at 4°C, resuspended in 12 ml of phosphate-buffered saline (PBS), and lysed by ultrasonication. Cell debris was sedimented by centrifugation, and the portion of the GST-fusion protein that remained in the supernatant was absorbed onto a glutathione-Sepharose 4B affinity matrix (GE Healthcare), and cleaved with PreScission protease (GE Healthcare) according to the manufacturer's protocol. The protein concentrations were determined as described previously (45), and sample purity was analyzed by SDS-PAGE.

HPLC analysis. Indole production in an enzymatic reaction was evaluated using reversed-phase high-performance liquid chromatography (HPLC) as pre-

viously described (30), with minor modifications. The reaction mixture contained the following reagents in a final volume of 100 μl: 167 mM potassium phosphate buffer (pH 7.5), 0.165 mM PLP, 0.2 mM reduced glutathione, 0.25 mg ml^{-1} bovine serum albumin (BSA), and 2 mM L-tryptophan with or without 100 μg ml^{-1} of the purified enzyme of *F. nucleatum* ATCC 25586. After layering with 100 μl of toluene, the mixture was incubated for 2 h at 37°C. A toluene aliquot (20 μl) from the sample was injected onto a C_{18} reversed-phase column (4.6 mm by 250 mm) (TSK-Gel ODS-80Ts; Tosoh, Tokyo, Japan). The mobile-phase solvent, 50% (vol/vol) methanol-water, was pumped through the column at a flow rate of 1 ml min^{-1} at 40°C. Excitation and emission wavelengths of 285 and 320 nm, respectively, were used.

Enzyme assay. L-Tryptophan degradation by purified tryptophanase was examined by measuring indole formation, as previously reported (40), with minor modifications. Briefly, after layering the reaction mixture (200 mM potassium buffer [pH 7.5], 0.165 mM PLP, 0.2 mM reduced glutathione, 0.25 mg ml^{-1} BSA, 10 μg ml^{-1} purified tryptophanase, and L-tryptophan) with 100 μl toluene, the reaction mixture was prewarmed for 5 min at 37°C. The reaction was initiated by adding a substrate solution. After 10 min of incubation, the reaction was terminated by the addition of 1 ml Ehrlich's reagent, which was prepared daily by mixing five volumes of 5% (wt/vol) *p*-dimethylaminobenzaldehyde in 95% (vol/vol) ethanol with 12 volumes of 5% (vol/vol) H_2SO_4 in 1-butanol. After incubation for 20 min at room temperature, the mixture was centrifuged at 15,000 × *g* for 2 min to remove insoluble materials. The supernatant was examined spectrophotometrically at 568 nm. The amounts of indole in each reaction mixture were calculated from a standard curve. Kinetic parameters were computed from a Lineweaver-Burk transformation of the Michaelis-Menten equation. The k_{cat} value was calculated from the V_{max} value and the molecular weight of *F. nucleatum* tryptophanase. Data were obtained from three independent experiments.

The degradation of *S*-ethyl-L-cysteine, *S*-methyl-L-cysteine, L-cysteine, L-alanine, and L-serine was measured by assaying pyruvate formation, as previously described (59). The assays were performed in 100-μl reaction mixtures containing 200 mM potassium phosphate buffer (pH 7.6), 0.165 mM PLP, 1 μg of purified enzyme, and several concentrations of each substrate. After 10 min of incubation at 37°C, reactions were terminated by adding 50 μl of 4.5% (vol/vol) trichloroacetic acid. The reaction mixtures were centrifuged, and 100 μl of the supernatants was added to 300 μl of 0.67 M sodium acetate (pH 5.2) containing 0.017% (wt/vol) 3-methyl-2-benzothiazolinone hydrazone. After incubation at 50°C for 30 min, the absorbance at 335 nm (A_{335}) was determined. The amounts of pyruvate were calculated from a standard curve prepared using crystalline sodium pyruvate. Data were obtained from three independent experiments.

Indole assay. Overnight cultures of *F. nucleatum* ATCC 25586 were diluted 1/20 in Columbia broth. Aliquots (1 ml) of the diluted samples were incubated in the wells of a flat-bottom 24-well polystyrene plate (Greiner Bio-One, Tokyo, Japan) with or without 1, 3, or 6 mM tryptophan for 48 h at 37°C. After the cell culture was centrifuged at 15,000 × *g* for 2 min and the bacterial pellet was removed, the supernatants of the samples were mixed immediately with 140 μl of Kovac's reagent (5% [wt/vol] *p*-dimethylamino-benzaldehyde, 75% [wt/vol] methanol, 2.5 M HCl). The indole concentration was measured spectrophotometrically from the A_{540} and calculated according to the standard curve.

Biofilm formation assay. Biofilm formation by *F. nucleatum* ATCC 25586 was assayed using a method described previously (35) with some modifications. Overnight cultures of *F. nucleatum* were diluted 1/20 in Columbia broth. Aliquots (200 μl) of the diluted samples were anaerobically incubated in the wells of a flat-bottom 96-well polyvinyl chloride (PVC) plate (BD Japan, Tokyo, Japan) with or without tryptophan (1, 3, or 6 mM) or indole (0.05, 0.1, 0.2, 0.4, 0.8, or 1.6 mM) for 48 h at 37°C. A portion (100 μl) of each cell culture was then transferred to a 96-well polystyrene plate and spectrophotometrically measured at 595 nm to assess planktonic bacterial growth. After discarding the remaining bacterial culture in the wells, bacterial cells bound to the wells were gently washed twice with PBS, air dried, and then stained with 200 μl of 0.1% (wt/vol) crystal violet for 15 min. After being washed 4 times with PBS to remove excess dye, the cell-bound dye was eluted using 200 μl of 99% methanol. Biofilm formation was quantified by measuring the A_{595}.

Confocal laser-scanning microscopy. Biofilms of *F. nucleatum* were formed on PVC sheets (5 × 5 mm) sunk in a 12-well plate containing Columbia broth with or without tryptophan (1, 3, or 6 mM) or indole (0.2 or 1.6 mM) for 48 h at 37°C. The biofilms formed on each sheet were washed twice with PBS to remove unbound cells, stained for 15 min in the dark with a drop of 5 mM SYTO9 (Invitrogen) in PBS, and rinsed twice with PBS. The sheet was then mounted on a drop of ProLong Gold (Invitrogen). Samples were observed using a confocal laser-scanning microscope (FV1000-D; Olympus, Tokyo, Japan) with an argon laser at 488 nm to excite the SYTO9 dye, and its fluorescence was gained through a 505- to 605-nm optical filter. Optical sections were collected with 2.5-μm steps through a sample depth of 70 μm. The three-dimensional structures of the biofilms were constructed using the Fluoview software (Olympus).

RESULTS

Organization of the *tnaA* homolog and the flanking regions in *F. nucleatum*. The DNA sequences of the *tnaA* homolog (*fn1943*) and flanking regions in *F. nucleatum* ATCC 25586 were obtained from the whole genome sequence of the strain (28) using GenBank (http://www.ncbi.nlm.nih.gov/). The open reading frame (ORF) (1,635 bp) is longer by at least 200 bp than the *tnaA* genes (1,389 to 1,416 bp) from other bacteria, such as *E. coli* (12), *P. vulgaris* (27), *H. influenza* (36), and *P. gingivalis* (61). The amino acid sequence deduced from *fn1943* of *F. nucleatum* displayed 28 to 34% identity with the *tnaA* sequences of the bacteria described above. In *E. coli*, the transcribed leader region of *tnaA* contains a 72-bp coding region, *tnaC*, for a 24-residue leader peptide (52), which is necessary for *tna* operon expression (20). In *F. nucleatum* ATCC 25586, no sequences corresponding to the leader peptide were found in the *fn1943* operon transcript (Fig. 1A), which was determined as described below. The upstream ORF from *fn1943*, namely, *fn1942*, existed in the opposite strand of the region, although homologous genes were not found in the corresponding region of *E. coli* or *P. gingivalis*. In contrast, the amino acid sequence of the gene downstream from *fn1943* of *F. nucleatum* ATCC 25586 (*fn1944*) was 15% identical to that of *tnaB* encoding low-affinity tryptophan permease in *E. coli* (18).

Transcriptional analyses of the *fn1943* region in *F. nucleatum*. Transcripts of the *fn1943* region in *F. nucleatum* ATCC 25586 were characterized using RT-PCR. The positions of the primer pairs designed to detect intergenic and intragenic regions are shown in Fig. 1A. No PCR product corresponding to the region spanning the borders of *fn1944*/*fn1945* were amplified (Fig. 1B), and *fn1942* expression was not detected. In contrast, PCR fragments corresponding to the region spanning the borders of *fn1943* and *fn1944* were amplified, with amplicons of the expected lengths. However, no products were amplified using cDNA prepared without reverse transcriptase, indicating that the RT-PCR products were not derived from contaminated chromosomal DNA (Fig. 1B). These results demonstrated that the *fn1943* and *fn1944* genes were cotranscribed as an operon in *F. nucleatum* ATCC 25586.

The transcription start site of *fn1943* in *F. nucleatum* ATCC 25586 was determined by 5′ RLM-RACE experiments using cDNA reverse transcribed from total RNA, which was extracted from *F. nucleatum* ATCC 25586 grown to the exponential phase. PCR fragments amplified with inner primers were subjected to DNA sequencing of the upstream region up to the transcription start site of *fn1943.* The junction of the adapter with *F. nucleatum* genomic DNA is the 5′ end of the transcript. Two forms of the *fn1943* transcript were detected, starting at adenine at positions −68 (in 4 of 11 plasmids analyzed) and −153 (in 7 of 11 plasmids analyzed) from the first nucleotide of the translation initiation codon of *fn1943* (Fig. 1C). Sequences similar to the consensus promoter, the −10 and −35 regions (23), were found in the regions upstream from both transcript starting positions.

Enzymatic characterization of the *fn1943* product of *F. nucleatum*. To characterize the product of the *fn1943* gene, we

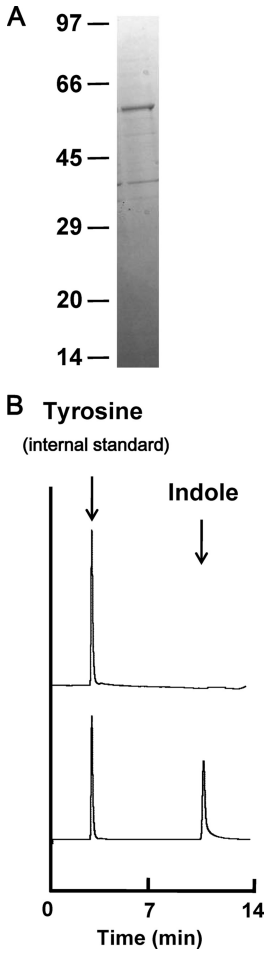

FIG. 2. Characterization of purified protein encoded by *fn1943* of *F. nucleatum* ATCC 25586. (A) SDS-PAGE analysis of recombinant Fn1943 of *F. nucleatum* ATCC 25586. Proteins were purified by affinity chromatography on glutathione-Sepharose 4B resin and digested with PreScission protease. The ~5-μg protein sample was subjected to SDS-PAGE and stained with Coomassie brilliant blue. Positions of molecular mass markers (in kDa) are shown. (B) Reversed-phase HPLC profiles of indole production from L-tryptophan by the purified Fn1943 of *F. nucleatum* ATCC 25586. A 2-μl aliquot of toluene that had been layered on the reaction mixture was injected onto a column with L-tyrosine as an internal standard. Reaction mixtures were prepared with (bottom) or without (top) recombinant Fn1943. Arrows indicate the elution positions of indole and tyrosine.

purified the recombinant protein using the pGEX-6P-1 vector system (Fig. 2A). The molecular mass of the denatured polypeptide agreed well with the predicted molecular mass (61 kDa).

HPLC analysis showed that incubation of the purified protein with L-tryptophan resulted in indole production, indicating that the *fn1943* gene encodes tryptophanase (Fig. 2B). Based on this result, we designated *fn1943* as *tnaA*. The kinetic activity of the recombinant tryptophanase was spectrophotometrically evaluated. The breakdown of substrates other than L-tryptophan was determined by assaying pyruvate production, since enzymatic degradation of the substrates invariably resulted in pyruvate formation. Our preliminary experiments showed that indole inhibited the assay using 3-methyl-2-benzothiazolinone hydrazone to detect pyruvate formation. Hence, the kinetic properties of the tryptophanase for L-tryptophan were determined by measuring the amounts of indole. The enzymatic properties of the purified enzyme are summarized in Table 2. The k_{cat} and k_{cat}/K_m values of the enzyme for L-tryptophan were much higher than those for *S*-methyl-L-cysteine or *S*-ethyl-L-cysteine. The enzyme had no detectable elimination activity with L-alanine, L-serine, or L-cysteine as a substrate.

TABLE 2. Steady-state kinetic parameters for TnaA from *F. nucleatum* ATCC 25586[a]

Substrate	K_m (mM)	k_{cat} (s^{-1})	k_{cat}/K_m (mM^{-1} s^{-1})
L-Tryptophan	0.26 ± 0.03	0.74 ± 0.04	2.79 ± 0.25
S-Methyl-L-cysteine	0.9 ± 0.19	0.11 ± 0.01	0.12 ± 0.002
S-Ethyl-L-cysteine	0.5 ± 0.06	0.4 ± 0.03	0.8 ± 0.04

[a] Values are means ± standard deviations from three experiments. No detectable elimination activity with l-alanine, l-serine, or l-cysteine as a substrate was observed.

Effect of the growth phase on *tnaA* expression. To examine the effect of the *F. nucleatum* growth phase on *tnaA* expression, real-time quantitative PCR analysis was performed. After the OD_{595} of cell cultures incubated for 4, 8, 12, and 24 h was measured to create a growth curve (Fig. 3), cDNA was prepared using total RNA extracted from each cell culture. The amounts of *tnaA* transcript in cells grown for 8 and 12 h were 12 and 9.7 times, respectively, larger than those for 4 h (early log phase). However, expression of the *tnaA* gene in the stationary phase (24 h) was only 5% of that in the early log phase (Fig. 3). The amounts of total cDNA were normalized using the housekeeping genes *fn0654* (phosphoglycerate kinase) and *fn2054* (glucose-6-phosphate isomerase; data not shown).

Effect of tryptophan on indole and *F. nucleatum* biofilm formation. The indole concentration was measured in a culture

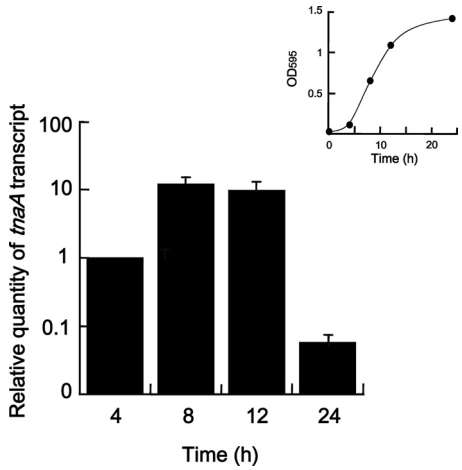

FIG. 3. Expression levels of *tnaA* in several cell growth phases of *F. nucleatum* ATCC 25586. The OD_{595} of cells incubated for 4, 8, 12, or 24 h for RNA extraction is indicated as an inset. The amounts of *tnaA* cDNA in each sample were analyzed by real-time quantitative PCR and are shown as relative values, after normalization using the housekeeping gene *fn0654*. Data are given as the means ± standard deviations from four experiments.

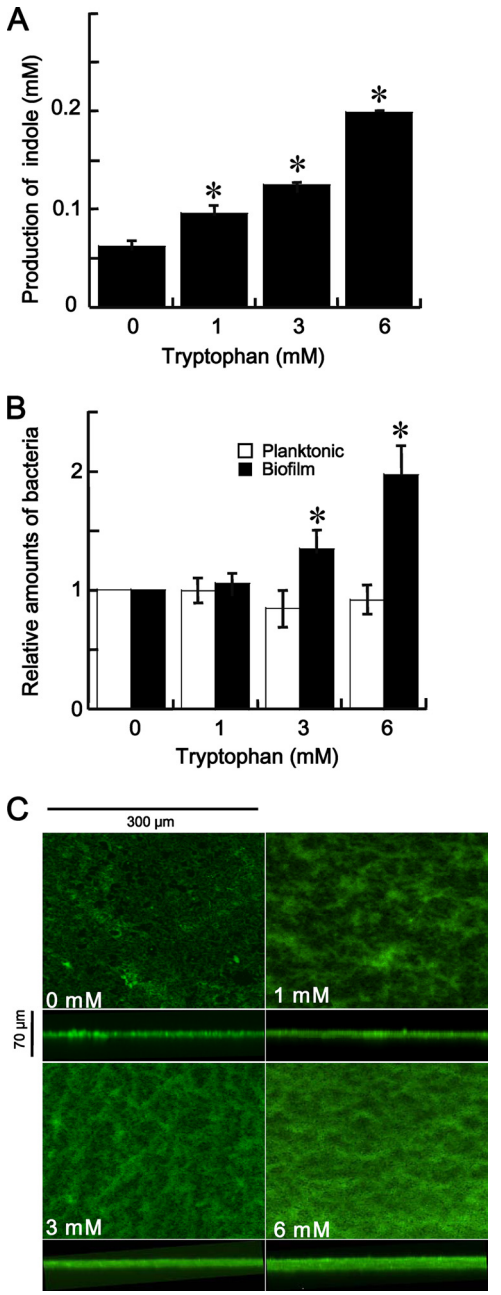

FIG. 4. Effects of tryptophan on indole production and biofilm formation by *F. nucleatum* ATCC 25586. (A) Indole production by *F. nucleatum* ATCC 25586 cells grown in the absence or presence of tryptophan; (B) relative amounts of planktonic and biofilm cells grown in the absence or presence of tryptophan. Bacteria were incubated for 48 h in 96-well PVC plates containing Columbia broth supplemented with or without 1, 3, or 6 mM tryptophan. The OD_{595} of the cell culture was measured to determine the amounts of planktonic cells. After cells were removed by centrifugation, the indole concentrations in the supernatants were measured. The amounts of biofilms were quantified using OD_{595} measurements following crystal violet staining and methanol elution. Data are given as the means ± standard deviations from three experiments. *, $P < 0.01$, *t* test. (C) Structure of *F. nucleatum* biofilms formed for 48 h with or without 1, 3, or 6 mM tryptophan. Biofilms formed on PVC sheets were stained with SYTO9 and observed by confocal laser-scanning microscopy. *x-z* reconstructions of each biofilm are shown below each *x-y* image.

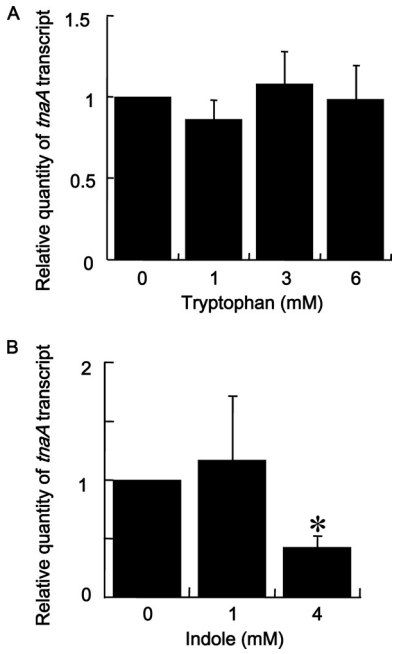

FIG. 5. Effect of tryptophan (A) and exogenous indole (B) on *tnaA* expression in *F. nucleatum*. Total RNA was extracted from *F. nucleatum* cells incubated for 8 h without indole and for another 1 h in the absence or presence of 1, 3, or 6 mM tryptophan or in the absence or presence of 1 or 4 mM indole. The relative amounts of *tnaA* in each cDNA sample were measured by real-time quantitative PCR analysis using *fn0654* to normalize the total cDNA. Data are given as means ± standard deviations from four experiments. *, $P < 0.01$, *t* test.

of *F. nucleatum* grown with tryptophan for 48 h. Addition of tryptophan into the bacterial cell culture increased the indole concentration in culture supernatants in a dose-dependent manner, although 0.06 mM indole was detected even in cell cultures grown without tryptophan (Fig. 4A).

Biofilm formation by *F. nucleatum* grown with tryptophan was also examined. The levels of biofilm formation on the flat bottoms of 96-well PVC plates were estimated by measuring the OD_{595} after staining the bacteria with crystal violet (Fig. 4B). The amount of biofilm formed by *F. nucleatum* also increased dose dependently with increasing tryptophan concentration. In contrast, the planktonic cells grown with or without various tryptophan concentrations were not significantly different. *F. nucleatum* biofilms formed on small PVC sheets in the presence or absence of tryptophan for 48 h were examined using confocal laser-scanning microscopy (Fig. 4C). The surface area of the PVC sheet that was covered with *F. nucleatum* biofilm was visually increased in accordance with the concentration of tryptophan added to the culture, reflecting the results obtained by the biofilm assay with crystal violet.

The effect of the addition of tryptophan on *tnaA* expression in *F. nucleatum* was also evaluated using real-time quantitative PCR (Fig. 5A). Cells were incubated for 8 h without tryptophan followed by incubation for another 1 h with or without 1, 3, or 6 mM tryptophan. The amounts of *tnaA* transcripts were not significantly different among *F. nucleatum* cells grown with or without tryptophan (Fig. 5A).

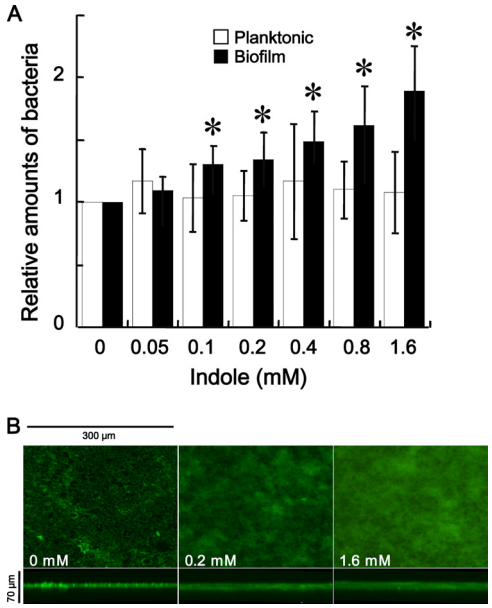

FIG. 6. Effects of exogenous indole on planktonic and biofilm cells of *F. nucleatum* ATCC 25586. (A) Relative amounts of planktonic and biofilm cells grown in the absence or presence of exogenous indole are shown. Bacteria were incubated for 48 h in 96-well PVC plates containing Columbia broth supplemented with or without 0.05, 0.1, 0.2, 0.4, 0.8, or 1.6 mM indole. The OD_{595} of the cell culture was measured to determine the amounts of planktonic cells. The amounts of biofilms were quantified using OD_{595} measurements following crystal violet staining and methanol elution. Data are given as the means ± standard deviations from three experiments. *, $P < 0.01$, *t* test. (B) Structure of *F. nucleatum* biofilms formed in absence or presence of 0.2 or 1.6 mM indole. Biofilms that formed on the PVC sheets were stained with SYTO9 and observed by confocal laser microscopy. *x-z* reconstructions of each biofilm are shown below each *x-y* image.

Effect of exogenous indole on biofilm formation and *tnaA* expression in *F. nucleatum*. The crystal violet biofilm assay revealed that *F. nucleatum* biofilm formation increased dose dependently with increasing exogenous indole (Fig. 6A). These findings were confirmed by confocal laser-scanning microscopy of biofilms formed in presence or absence of 0.2 or 1.6 mM indole (Fig. 6B). In contrast, planktonic cells grown without indole were not significantly different from those grown with any tested concentration of indole (Fig. 6A).

The effect of exogenous indole on *tnaA* expression in *F. nucleatum* was also evaluated using real-time quantitative PCR (Fig. 5B). Cells were incubated for 8 h without indole followed by further incubation for 1 h with or without 1 or 4 mM indole. There was no significant difference in the amounts of *tnaA* between *F. nucleatum* cells incubated with or without 1 mM indole. However, when cells were incubated with 4 mM indole, the *tnaA* expression was decreased to ~43% compared to control. Similar results were obtained regardless of whether the amounts of total cDNA were normalized using the housekeeping gene *fn0654* or *fn2054*.

DISCUSSION

Until the tryptophanase of *P. gingivalis* was recently reported (61), the mechanism by which indole was produced by oral microorganisms had not been examined in much detail. This is probably because the importance of indole had not been recognized, except for its usefulness as a common diagnostic marker. However, increasing evidence suggests that indole mediates cell-to-cell signaling, similar to the N-acyl derivatives of homoserine lactone, cyclic peptide, and quinolones (9, 34, 41, 55). The goal of this study was to gain insight into indole production by *F. nucleatum*, a key microorganism for dental biofilm formation, and to evaluate the effects of tryptophan and indole on biofilm formation.

The *tna* operon of *E. coli* contains two major structural genes, *tnaA* and *tnaB* (12). The former gene is preceded by a 319-bp transcribed leader region, *tnaL*, which contains a short coding region, *tnaC*. In *P. gingivalis*, the flanking regions of *tnaA* do not contain *tnaB* or *tnaC* (61). As seen in the *tna* operon of *E. coli*, the *tnaA* gene was cotranscribed with *tnaB* in *F. nucleatum*. However, the transcription start site of the *tna* operon in *F. nucleatum* ATCC 25586 was 67 or 152 bp upstream from the initiation codon of *tnaA* (Fig. 1C), revealing that the region corresponding to *tnaL* in *F. nucleatum* was much shorter than that in *E. coli.* No sequence homologous with *tnaC* was found in the *tnaL* region of *F. nucleatum* ATCC 25586. Furthermore, no sequence was found that bound to the cyclic AMP (cAMP) receptor protein, which is proximal to the transcription start site of the *tna* operon in *E. coli* and associated with *tnaA* operon expression (13). These findings suggest that *tna* operon regulation in *F. nucleatum* is different from that in *E. coli*.

The K_m value (0.26 ± 0.03 mM) of *F. nucleatum* tryptophanase for L-tryptophan was slightly lower than that of *E. coli* (0.32 mM) (43, 56) or *B. alvei* (0.27 mM) (25) but slightly higher than that of *P. gingivalis* (0.20 mM) (61). These findings indicate that the affinity of *F. nucleatum* tryptophanase to L-tryptophan was similar to those of tryptophanases of other bacteria. In contrast, the k_{cat} and k_{cat}/K_m values (0.74 ± 0.04 s^{-1} and 2.79 ± 0.25 mM^{-1} s^{-1}, respectively) were less than those in *E. coli* (6.8 s^{-1} and 30 mM^{-1} s^{-1}, respectively) (46) and *P. gingivalis* (1.37 s^{-1} and 6.87 mM^{-1} s^{-1}, respectively). Thus, the capacity of tryptophanase from *F. nucleatum* to produce indole was lower than that of tryptophanase from *E. coli* or *P. gingivalis*.

Neither tryptophanase from *F. nucleatum* nor that from *P. gingivalis* (61) degraded L-serine or L-cysteine, both of which were degraded by tryptophanases from *E. coli* (40) and *P. vulgaris* (62). Since the amino acid identity between tryptophanase from *F. nucleatum* and that from *P. gingivalis* was nearly identical to that between tryptophanase from *F. nucleatum* and those from the other bacteria described above, some specific amino acids in tryptophanase might play an important role in determining the enzyme substrate specificity. In addition to previous reports describing the amino acids associated with the active site of the enzyme (14–16, 32), further studies on which amino acids determine the substrate specificity would be interesting.

The evidence that indole is a cell-to-cell signaling molecule influencing bacterial biofilm formation is rather complicated. In *E. coli*, indole represses biofilm formation by inducing the quorum-sensing signal autoinducer I (34). Indole increases *Vibrio cholerae* biofilms by activating genes involved in *Vibrio* polysaccharide production, which is essential for biofilm for-

mation in the bacteria (41). We demonstrated that *F. nucleatum* biofilms were increased in accordance with the amounts of indole (Fig. 6A) or tryptophan (Fig. 4B) added to the media. The latter finding is likely due to indole production from tryptophan by tryptophanase. Indeed, the indole concentration was increased by the addition of tryptophan to the bacterial cultures.

The physiological indole concentration seen in stationary-phase supernatants of *E. coli* is 0.3 mM (55), which is high enough to increase biofilm formation by *F. nucleatum*. Incubation of *F. nucleatum* with 6 mM tryptophan, at which *F. nucleatum* biofilms were significantly increased (Fig. 4B), resulted in production of approximately 0.2 mM indole (Fig. 4A). In contrast, the *F. nucleatum* biofilms were efficiently increased by the presence of 0.2 mM indole (Fig. 6A). Interestingly, the *F. nucleatum* biofilms formed in the presence of 6 mM tryptophan were quantitatively more than those in the presence of 0.2 mM indole (Fig. 4C and 6B), suggesting that the biofilm development may be influenced not only by indole but also by tryptophan, or its metabolites. However, the mechanism by which indole and tryptophan increase *F. nucleatum* biofilm formation is unclear. Studies on indole- or tryptophan-mediated gene regulation using microarrays (41) and two-dimensional electrophoresis (9) might provide useful information to elucidate the mechanism.

Real-time quantitative PCR analysis revealed approximately 10 and 100 times more *F. nucleatum tnaA* transcripts in the mid- or late-log-phase cells than in the early-log-phase or stationary-phase cells, respectively (Fig. 3). The relatively low stationary-phase expression of *tnaA* agrees with a previous report showing that *tnaA* was repressed 13-fold in 6-day-old *E. coli* biofilms (48). Interestingly, addition of tryptophan even at a very high concentration (6 mM), at which indole was produced at 0.23 mM in the *F. nucleatum* culture, did not affect *tnaA* expression (Fig. 5A). This might be because the *F. nucleatum tnaA* region contains the *tnaC* sequence, which is associated with the tryptophan-induced inhibition of Rho factor-dependent transcription termination (53). In contrast, the decreased *tnaA* level at high indole concentrations seemed to be associated with the feedback response (Fig. 5B).

Certain periodontopathogenic bacteria, including *P. gingivalis*, *Prevotella intermedia*, and *F. nucleatum*, are able to produce indole from L-tryptophan (17). It was reported more than 50 years ago that saliva from patients with periodontal disease produced more indole than saliva from periodontally healthy subjects (3). However, it is unclear whether the indole toxicity is directly associated with periodontal disease, whereas *F. nucleatum* biofilms were increased in the presence of indole (Fig. 6A). It should be noted that PVC was used as a substrate for *F. nucleatum* biofilms in this study. Our preliminary experiments showed that the plates and sheets made of PVC, which have been frequently employed in similar experiments, fix *F. nucleatum* biofilms more firmly than those of other artificial substrates, including polystyrene. However, such plates and sheets do not necessarily reflect the conditions in the oral cavity, since the scaffold on which bacterial biofilms are experimentally formed can generally influence their amount and structure. In addition, natural biofilms such as dental plaque are complex structures of multiple organisms which may behave quite differently from monoculture biofilms due to cell-to-cell signaling molecules. The function of indole as an interspecies signal that decreases *E. coli* and increases *Pseudomonas* sp. biofilms (34) is interesting, given that *F. nucleatum* is an important central microorganism in oral biofilms (29). In contrast, tryptophan metabolism and indole production in *F. nucleatum* may also be influenced by cell-to-cell signaling molecules that the other bacteria produce. Thus, more comprehensive studies are necessary to precisely understand the effect of indole on the biofilm formation by *F. nucleatum* and the other bacteria in the human oral cavity.

ACKNOWLEDGMENTS

This study was supported in part by a Research Grant for Promoting Technological Seeds (Y.Y.) and by Grants-in-Aid for Scientific Research (no. 20592463, 20592181, and 21592631) from the Ministry of Education, Culture, Sports, Science and Technology, Japan.

REFERENCES

1. **Anyanful, A., J. M. Dolan-Livengood, T. Lewis, S. Sheth, M. N. Dezalia, M. A. Sherman, L. V. Kalman, G. M. Benian, and D. Kalman.** 2005. Paralysis and killing of *Caenorhabditis elegans* by enteropathogenic *Escherichia coli* requires the bacterial tryptophanase gene. Mol. Microbiol. **57:**988–1007.
2. **Bauer, C., D. Schoonbroodt, C. Wagner, and Y. Horsmans.** 2000. Liver abscesses due to *Fusobacterium* species. Liver **20:**267–268.
3. **Berg, M., D. Y. Burrill, and L. S. Fosdick.** 1946. Chemical studies in periodontal disease. III. Putrefaction of salivary proteins. J. Dent. Res. **25:**231–246.
4. **Bolstad, A. I., H. B. Jensen, and V. Bakken.** 1996. Taxonomy, biology, and periodontal aspects of *Fusobacterium nucleatum*. Clin. Microbiol. Rev. **9:**55–71.
5. **Botha, S. J., R. Senekal, P. L. Steyn, and W. J. Coetzee.** 1993. Anaerobic bacteria in orofacial abscesses. J. Dent. Assoc. S. Afr. **48:**445–449.
6. **Brook, I., and E. H. Frazier.** 2000. Aerobic and anaerobic microbiology in intra-abdominal infections associated with diverticulitis. J. Med. Microbiol. **49:**827–830.
7. **Chant, E. L., and D. K. Summers.** 2007. Indole signalling contributes to the stable maintenance of *Escherichia coli* multicopy plasmids. Mol. Microbiol. **63:**35–43.
8. **Chaudhry, R., B. Dhawan, B. V. Laxmi, and V. S. Mehta.** 1998. The microbial spectrum of brain abscess with special reference to anaerobic bacteria. Br. J. Neurosurg. **12:**127–130.
9. **Collet, A., S. Vilain, P. Cosette, G. A. Junter, T. Jouenne, R. S. Phillips, and P. Di Martino.** 2007. Protein expression in *Escherichia coli* S17-1 biofilms: impact of indole. Antonie Van Leeuwenhoek **91:**71–85.
10. **Cowell, J. L., and R. D. DeMoss.** 1973. Trytophanase from *Aeromonas liquefaciens*. Subunit structure and aggregation of the enzyme into enzymatically active polymeric species. J. Biol. Chem. **248:**6262–6269.
11. **Debelian, G. J., I. Olsen, and L. Tronstad.** 1998. Anaerobic bacteremia and fungemia in patients undergoing endodontic therapy: an overview. Ann. Periodontol. **3:**281–287.
12. **Deeley, M. C., and C. Yanofsky.** 1981. Nucleotide sequence of the structural gene for tryptophanase of *Escherichia coli* K-12. J. Bacteriol. **147:**787–796.
13. **Deeley, M. C., and C. Yanofsky.** 1982. Transcription initiation at the tryptophanase promoter of *Escherichia coli* K-12. J. Bacteriol. **151:**942–951.
14. **Demidkina, T. V., M. V. Barbolina, N. G. Faleev, B. Sundararaju, P. D. Gollnick, and R. S. Phillips.** 2002. Threonine-124 and phenylalanine-448 in *Citrobacter freundii* tyrosine phenol-lyase are necessary for activity with L-tyrosine. Biochem. J. **363:**745–752.
15. **Demidkina, T. V., N. G. Faleev, A. I. Papisova, N. P. Bazhulina, V. V. Kulikova, P. D. Gollnick, and R. S. Phillips.** 2006. Aspartic acid 214 in *Citrobacter freundii* tyrosine phenol-lyase ensures sufficient C-H-acidity of the external aldimine intermediate and proper orientation of the cofactor at the active site. Biochim. Biophys. Acta **1764:**1268–1276.
16. **Demidkina, T. V., L. N. Zakomirdina, V. V. Kulikova, I. S. Dementieva, N. G. Faleev, L. Ronda, A. Mozzarelli, P. D. Gollnick, and R. S. Phillips.** 2003. Role of aspartate-133 and histidine-458 in the mechanism of tryptophan indole-lyase from *Proteus vulgaris*. Biochemistry **42:**11161–11169.
17. **Duerden, B. I., J. G. Collee, R. Brown, A. G. Deacon, and W. P. Holbrook.** 1980. A scheme for the identification of clinical isolates of Gram-negative anaerobic bacilli by conventional bacteriological tests. J. Med. Microbiol. **13:**231–245.
18. **Edwards, R. M., and M. D. Yudkin.** 1982. Location of the gene for the low-affinity tryptophan-specific permease of *Escherichia coli*. Biochem. J. **204:**617–619.
19. **Gong, F., K. Ito, Y. Nakamura, and C. Yanofsky.** 2001. The mechanism of tryptophan induction of tryptophanase operon expression: tryptophan inhib-

its release factor-mediated cleavage of TnaC-peptidyl-tRNA^{Pro}. Proc. Natl. Acad. Sci. U. S. A. **98:**8997–9001.
20. **Gong, F., and C. Yanofsky.** 2002. Analysis of tryptophanase operon expression in vitro: accumulation of TnaC-peptidyl-tRNA in a release factor 2-depleted S-30 extract prevents Rho factor action, simulating induction. J. Biol. Chem. **277:**17095–17100.
21. **Gong, F., and C. Yanofsky.** 2002. Instruction of translating ribosome by nascent peptide. Science **297:**1864–1867.
22. **Gong, F., and C. Yanofsky.** 2001. Reproducing tna operon regulation in vitro in an S-30 system. Tryptophan induction inhibits cleavage of TnaC peptidyl-tRNA. J. Biol. Chem. **276:**1974–1983.
23. **Hawley, D. K., and W. R. McClure.** 1983. Compilation and analysis of *Escherichia coli* promoter DNA sequences. Nucleic Acids Res. **11:**2237–2255.
24. **Hirakawa, H., Y. Inazumi, T. Masaki, T. Hirata, and A. Yamaguchi.** 2005. Indole induces the expression of multidrug exporter genes in *Escherichia coli*. Mol. Microbiol. **55:**1113–1126.
25. **Hoch, J. A., F. J. Simpson, and R. D. DeMoss.** 1966. Purification and some properties of tryptophanase from *Bacillus alvei*. Biochemistry **5:**2229–2237.
26. **Hockensmith, M. L., D. L. Mellman, and E. L. Aronsen.** 1999. *Fusobacterium nucleatum* empyema necessitans. Clin. Infect. Dis. **29:**1596–1598.
27. **Kamath, A. V., and C. Yanofsky.** 1992. Characterization of the tryptophanase operon of *Proteus vulgaris*. Cloning, nucleotide sequence, amino acid homology, and in vitro synthesis of the leader peptide and regulatory analysis. J. Biol. Chem. **267:**19978–19985.
28. **Kapatral, V., I. Anderson, N. Ivanova, G. Reznik, T. Los, A. Lykidis, A. Bhattacharyya, A. Bartman, W. Gardner, G. Grechkin, L. Zhu, O. Vasieva, L. Chu, Y. Kogan, O. Chaga, E. Goltsman, A. Bernal, N. Larsen, M. D'Souza, T. Walunas, G. Pusch, R. Haselkorn, M. Fonstein, N. Kyrpides, and R. Overbeek.** 2002. Genome sequence and analysis of the oral bacterium *Fusobacterium nucleatum* strain ATCC 25586. J. Bacteriol. **184:**2005–2018.
29. **Kolenbrander, P. E., R. N. Andersen, D. S. Blehert, P. G. Egland, J. S. Foster, and R. J. Palmer, Jr.** 2002. Communication among oral bacteria. Microbiol. Mol. Biol. Rev. **66:**486–505.
30. **Krstulovic, A. M., and C. Matzura.** 1979. Rapid assay for tryptophanase using reversed-phase high-performance liquid chromatography. J. Chromatogr. **176:**217–224.
31. **Ku, S. Y., P. Yip, and P. L. Howell.** 2006. Structure of *Escherichia coli* tryptophanase. Acta Crystallogr. D Biol. Crystallogr. **62:**814–823.
32. **Kulikova, V. V., L. N. Zakomirdina, I. S. Dementieva, R. S. Phillips, P. D. Gollnick, T. V. Demidkina, and N. G. Faleev.** 2006. Tryptophanase from *Proteus vulgaris*: the conformational rearrangement in the active site, induced by the mutation of tyrosine 72 to phenylalanine, and its mechanistic consequences. Biochim. Biophys. Acta **1764:**750–757.
33. **Lark, R. L., S. A. McNeil, K. VanderHyde, Z. Noorani, J. Uberti, and C. Chenoweth.** 2001. Risk factors for anaerobic bloodstream infections in bone marrow transplant recipients. Clin. Infect. Dis. **33:**338–343.
34. **Lee, J., A. Jayaraman, and T. K. Wood.** 2007. Indole is an inter-species biofilm signal mediated by SdiA. BMC Microbiol. **7:**42.
35. **Loo, C. Y., D. A. Corliss, and N. Ganeshkumar.** 2000. *Streptococcus gordonii* biofilm formation: identification of genes that code for biofilm phenotypes. J. Bacteriol. **182:**1374–1382.
36. **Martin, K., G. Morlin, A. Smith, A. Nordyke, A. Eisenstark, and M. Golomb.** 1998. The tryptophanase gene cluster of *Haemophilus influenzae* type b: evidence for horizontal gene transfer. J. Bacteriol. **180:**107–118.
37. **Martino, P. D., R. Fursy, L. Bret, B. Sundararaju, and R. S. Phillips.** 2003. Indole can act as an extracellular signal to regulate biofilm formation of *Escherichia coli* and other indole-producing bacteria. Can. J. Microbiol. **49:**443–449.
38. **Martius, J., and D. A. Eschenbach.** 1990. The role of bacterial vaginosis as a cause of amniotic fluid infection, chorioamnionitis and prematurity—a review. Arch. Gynecol. Obstet. **247:**1–13.
39. **Moore, W. E., and L. V. Moore.** 1994. The bacteria of periodontal diseases. Periodontol. 2000 **5:**66–77.
40. **Morino, Y., and E. E. Snell.** 1970. Tryptophanase (*Escherichia coli* B). Methods Enzymol. **17A:**439–446.
41. **Mueller, R. S., S. Beyhan, S. G. Saini, F. H. Yildiz, and D. H. Bartlett.** 2009. Indole acts as an extracellular cue regulating gene expression in *Vibrio cholerae*. J. Bacteriol. **191:**3504–3516.
42. **Nakano, Y., Y. Yoshida, Y. Yamashita, and T. Koga.** 1995. Construction of a series of pACYC-derived plasmid vectors. Gene **162:**157–158.
43. **Newton, W. A., Y. Morino, and E. E. Snell.** 1965. Properties of crystalline tryptophanase. J. Biol. Chem. **240:**1211–1218.
44. **Newton, W. A., and E. E. Snell.** 1964. Catalytic properties of tryptophanase, a multifunctional pyridoxal phosphate enzyme. Proc. Natl. Acad. Sci. U. S. A. **51:**382–389.
45. **Pace, C. N., F. Vajdos, L. Fee, G. Grimsley, and T. Gray.** 1995. How to measure and predict the molar absorption coefficient of a protein. Protein Sci. **4:**2411–2423.
46. **Phillips, R. S., and P. D. Gollnick.** 1989. Evidence that cysteine 298 is in the active site of tryptophan indole-lyase. J. Biol. Chem. **264:**10627–10632.
47. **Qi, M., K. E. Nelson, S. C. Daugherty, W. C. Nelson, I. R. Hance, M. Morrison, and C. W. Forsberg.** 2005. Novel molecular features of the fibrolytic intestinal bacterium *Fibrobacter intestinalis* not shared with *Fibrobacter succinogenes* as determined by suppressive subtractive hybridization. J. Bacteriol. **187:**3739–3751.
48. **Ren, D., L. A. Bedzyk, S. M. Thomas, R. W. Ye, and T. K. Wood.** 2004. Gene expression in *Escherichia coli* biofilms. Appl. Microbiol. Biotechnol. **64:**515–524.
49. **Shine, J., and L. Dalgarno.** 1974. The 3′-terminal sequence of *Escherichia coli* 16S ribosomal RNA: complementarity to nonsense triplets and ribosome binding sites. Proc. Natl. Acad. Sci. U. S. A. **71:**1342–1346.
50. **Snell, E. E.** 1975. Tryptophanase: structure, catalytic activities, and mechanism of action. Adv. Enzymol. Relat. Areas Mol. Biol. **42:**287–333.
51. **Stewart, V., R. Landick, and C. Yanofsky.** 1986. Rho-dependent transcription termination in the tryptophanase operon leader region of *Escherichia coli* K-12. J. Bacteriol. **166:**217–223.
52. **Stewart, V., and C. Yanofsky.** 1985. Evidence for transcription antitermination control of tryptophanase operon expression in *Escherichia coli* K-12. J. Bacteriol. **164:**731–740.
53. **Stewart, V., and C. Yanofsky.** 1986. Role of leader peptide synthesis in tryptophanase operon expression in *Escherichia coli* K-12. J. Bacteriol. **167:**383–386.
54. **Tso, W. W., and J. Adler.** 1974. Negative chemotaxis in *Escherichia coli*. J. Bacteriol. **118:**560–576.
55. **Wang, D., X. Ding, and P. N. Rather.** 2001. Indole can act as an extracellular signal in *Escherichia coli*. J. Bacteriol. **183:**4210–4216.
56. **Watanabe, T., and E. E. Snell.** 1977. The interaction of *Escherichia coli* tryptophanase with various amino and their analogs. Active site mapping. J. Biochem. **82:**733–745.
57. **Yanofsky, C.** 2007. RNA-based regulation of genes of tryptophan synthesis and degradation, in bacteria. RNA **13:**1141–1154.
58. **Yoshida, H., H. Kumagai, and H. Yamada.** 1974. Crystalline holotryptophanase from *Proteus rettgeri*. FEBS Lett. **48:**56–59.
59. **Yoshida, Y., Y. Nakano, A. Amano, M. Yoshimura, H. Fukamachi, T. Oho, and T. Koga.** 2002. *lcd* from *Streptoccus anginosus* encodes a C-S lyase with α,β-elimination activity that degrades L-cysteine. Microbiology **148:**3961–3970.
60. **Yoshida, Y., M. Negishi, and Y. Nakano.** 2003. Homocysteine biosynthesis pathways of *Streptococcus anginosus*. FEMS Microbiol. Lett. **221:**277–284.
61. **Yoshida, Y., T. Sasaki, S. Ito, H. Tamura, K. Kunimatsu, and H. Kato.** 2009. Identification and molecular characterization of tryptophanase encoded by *tnaA* in *Porphyromonas gingivalis*. Microbiology **155:**968–978.
62. **Zakomirdina, L. N., V. V. Kulikova, O. I. Gogoleva, I. S. Dementieva, N. G. Faleev, and T. V. Demidkina.** 2002. Tryptophan indole-lyase from *Proteus vulgaris*: kinetic and spectral properties. Biochemistry (Mosc.) **67:**1189–1196.